Fast Spiral Magnetic Resonance Imaging with Trapezoidal Gradients

Jeff H. Duyn[1] and Yihong Yang

Laboratory of Diagnostic Radiology Research, OIR, National Institutes of Health Building 10, Room B1N-256, Bethesda, Maryland 20892

A modified spiral imaging technique is presented, in which the conventional sinusoidal gradient waveforms are replaced by trapezoidal ones. In addition to allowing a reduced data acquisition time, the new waveforms circumvent specific hardware restrictions on the minimum scan repetition time. © 1997 Academic Press

Key Words: fast MRI; spiral MRI; gradient slew rate; duty cycle.

INTRODUCTION

Spiral MRI allows fast scanning with excellent SNR, and is relatively insensitive to motion (*1–3*). Applications include cardiac imaging (*1*), as well as functional neuroimaging (fMRI) based on blood oxygenation (BOLD) dependent contrast (*3–5*). Due to the particular design of gradient waveforms, not every clinical scanner allows straightforward implementation of spiral scan. In particular, a single-shot spiral scan puts high demands on gradient hardware, requiring careful design of gradient waveforms.

One hardware limitation of some clinical scanners is the ramping duty cycle. This duty cycle limit relates to the percentage of scan time spent with ramping (altering) the gradient amplitude, and stems from restrictions on the amount of heat dissipated by the pulse-width modulator controlling the output voltage of the gradient amplifier. This type of gradient amplifier limitation is particularly restrictive for spiral scan, in which the gradient amplitude continuously changes during data collection.

One approach in overcoming the conditions imposed by the gradient amplifiers is modification of the spiral design, e.g., by using a piecewise linear trajectory (*6*). This approach can significantly reduce ramping duty cycles, in particular for amplitude limited waveform designs. However, it results in only a small improvement for slew rate (SR) limited designs, such as used for single-shot imaging. In the following we will demonstrate improvements attainable with an alternative design, in which the sinusoidal gradient lobes are replaced by trapezoids. Earlier implementations were aimed at obtaining rectilinear *k*-space trajectories (*7*) or at

allowing easier implementation on scanner hardware (*8*). The current gradient waveform provides the desired reduction in ramping duty cycle, without significant reduction in scan duration or sampling uniformity of *k*-space.

METHODS

Theory

The constant (maximum) slew rate design for spirals with equidistant spacing of the revolutions (Archimedian spirals) is in first approximation characterized by (*9*)

$$G_x(t) = a_1 \cdot t^{1/3} \cdot \sin(a_2 \cdot t^{2/3})$$
$$G_y(t) = a_1 \cdot t^{1/3} \cdot \cos(a_2 \cdot t^{2/3}), \qquad [1]$$

with

$$a_1 = \frac{3}{2} \frac{SR}{a_2}, \; a_2 = \frac{n \cdot \pi}{T_{\mathrm{acq}}^{2/3}},$$

SR the maximum available slew rate, and *n* the image matrix size (twice the number of spiral revolutions). T_{acq} is the duration of the data acquisition window (equivalent to duration of spiral waveform), determined by

$$T_{\mathrm{acq}} = \frac{2 \cdot \pi^{3/2} \cdot n}{3 \cdot \sqrt{SR \cdot p}}, \qquad [2]$$

with *p* the nominal pixel size (spatial resolution).

This design, in which the vector sum of the slew rates is constant, allows multishot imaging by interleaving (*10*) through rotation of the gradient waveforms over an arbitrary angle. For single-shot imaging, in which no rotation of the waveforms is required, this design criterion appears too stringent. In this particular case, we are allowed to employ the maximum slew rate on both G_x and G_y waveforms simultaneously, and replace the (damped) sinusoidal gradient lobes by triangles or trapezoids. This can provide for a reduced ramping duty cycle, as well as a reduced T_{acq}. Disadvantages are a reduced sampling uniformity of *k*-space, and an in-

creased likelihood of eddy-current effects. In the following, we will focus on reduction of the ramping duty cycle, while keeping distortion of the k-space trajectory at minimum.

Replacing the sinusoidal gradient lobes by trapezoids affects the k-space trajectory. In order to maintain constant distance between the ''spiral'' revolutions, we propose the use of congruent trapezoids:

$$G_x(t) = \sum_{i=1}^{n} b_1 \cdot (-1)^i \cdot \left(\frac{(i-0.5)\cdot\pi}{b_2} \right)^{1/2}$$

$$\times \text{TRAP}_r\left(\left(\frac{(i-1)\cdot\pi}{b_2} \right)^{3/2}, \left(\frac{i\cdot\pi}{b_2} \right)^{3/2} \right)$$

$$G_y(t) = \sum_{i=1}^{n} b_1 \cdot (-1)^i \cdot \left(\frac{i\cdot\pi}{b_2} \right)^{1/2}$$

$$\times \text{TRAP}_r\left(\left(\frac{(i-0.5)\cdot\pi}{b_2} \right)^{3/2}, \right.$$

$$\left. \times \left(\frac{(i+0.5)\cdot\pi}{b_2} \right)^{3/2} \right). \qquad [3]$$

$\Sigma_i \, q_1(i) \cdot \text{TRAP}_r(q_2(i), q_3(i))$ indicates a concatenation of trapezoids with amplitudes $q_1(i)$, starting and ending at $q_2(i)$ and $q_3(i)$, respectively, with each trapezoid having a fraction r (same for all trapezoids) of its duration spent on ramps (at the maximum slew rate SR). The index i relates to the revolution number in k-space, and relates to t according to $i \approx t^{2/3}$, a relationship equivalent to Eq. [1]. For constant T_{acq}, and approximating the gradient lobes in [1] with pure sinusoids, we find

$$b_1 = \frac{8}{\pi^2 \cdot (2 \cdot r - r^2)} \cdot a_1,$$

$$b_2 = a_2. \qquad [4]$$

An example of a trapezoidal waveform design is given in Figs. 1a and 1b. By varying the ramp fraction r, we can manipulate the ramping duty cycle, as well as the trajectory. For example, $r = 0.1$ results in square-looking spirals (Fig. 1c), whereas at $r = 0.56$ (Fig. 1d), the trajectory approaches the circular character of sinusoidal waveforms (Fig. 1e). The corresponding sampling densities of both trapezoidal designs and sinusoidal waveforms are compared in Figs. 1f, 1g, and 1h, respectively. With trapezoidal scanning, the sampling density is somewhat reduced, theoretically resulting in a less uniform distribution of SNR over the spatial frequencies. Table 1 gives some calculated characteristics for a range of r values, at $n = 64$, and $p = 3.75$ mm, and a constant T_{acq} of 22 ms. The amplitude of the gradient waveforms is adjusted to obtain equal k-space coverage (surface area) for all designs, resulting in comparable effec-

tive resolutions. The ''shape'' parameter in the table was determined from the circumference of the area covered in k-space, and indicates the maximum deviation (radial distance) from a circular circumference (with equal coverage).

Although interleaving of the noncircular trapezoidal trajectories cannot be realized by simple rotation, it can be done by adjusting the amplitudes of the individual trapezoids (an extra amplitude factor proportional to $i^{-0.5}$ in (*3*)). An example of a 2-interleave design is given in Fig. 1i.

MR Experiments

MR experiments were performed on a 1.5-T GE-SIGNA echo speed scanner (General Electric, Milwaukee, WI), running at the EPIC 5.5 platform. The specifications for the GE actively shielded whole-body gradient set were slew rate 120 $T.m^{-1}.s^{-1}$, ramping duty cycle 25%, and maximum gradient strength 2.2 $G.cm^{-1}$. Eddy-current compensation was performed using the manufacturer-supplied, built-in adjustment package. Multislice single-shot spiral scanning (*11*) was performed on normal subjects. The studies were performed as part of a protocol at the National Institutes of Health, approved by the Intramural Review Board. Image quality (presence of artifacts, and effective resolution) was evaluated with repeated scans, using TE/TR = 25/100 ms (acquisition time = 3.6 s for 36 slices). Scan-to-scan signal stability, an important issue in, e.g., f MRI experiments, was determined with TR = 50 ms (acquisition time = 1.8 s for 36 slices). For this purpose, an insertable gradient/RF coil assembly (Medical Advances, Milwaukee, WI) was used to allow the increased ramping duty cycle needed for the comparison with the standard sinusoidal gradient waveforms.

Data Processing

The spiral k-space data were re-sampled to an orthogonal equidistant grid using a regridding algorithm with a Gaussian convolution window (*12*). Apodization was performed using a radial cosine filter (*11*). On the time-series data, correction for rigid body motion between scans was performed using a multiresolution least-squares difference algorithm with cubic spline interpolation (*13, 14*). The theoretical in-plane resolution, calculated from the area of the simulated 2D point-spread function (PSF) at half of its peak magnitude, was 1.88 pixel^2 (equivalent to 1.37 pixels width of rectangular PSF). The image resolution of the actual data was estimated using the time-series data by computing the full width at half maximum (FWHM) of the spatial autocorrelation (*15, 16*). This estimate assumes a Gaussian noise distribution within the images. The scan-to-scan stability was determined from the standard deviation of the image intensity time course on a pixel-by-pixel basis (*5*).
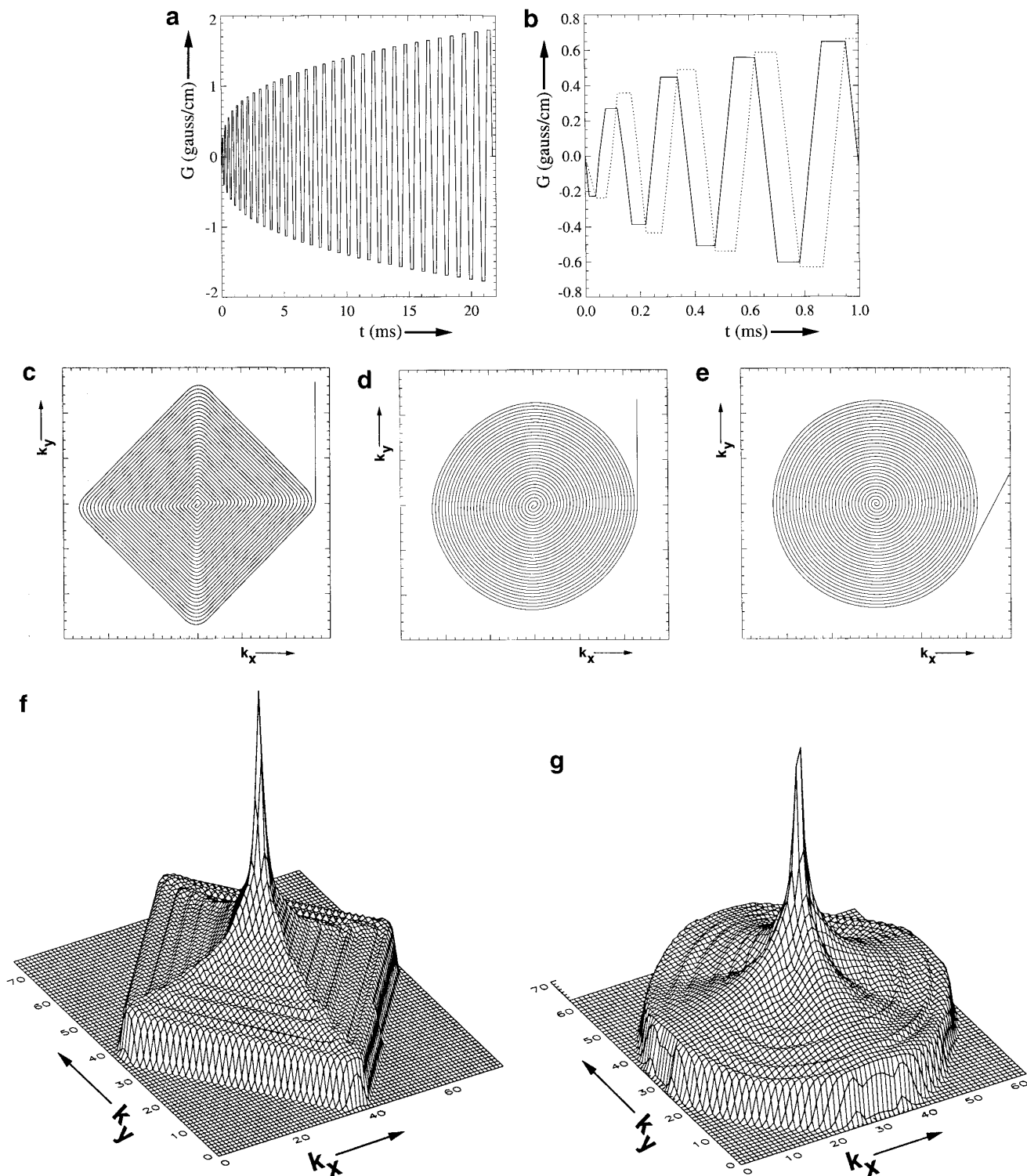
FIG. 1. Examples of trapezoidal designs. The gradient waveform (single axis) for a 22-ms trapezoidal design ($r = 0.50$) is given in (a), whereas (b) indicates the gradient switching on both axes (dashes and dotted lines) for the early part (first millisecond) of this design. Small amplitude adjustment were made on the first few gradient lobes to improve k-space uniformity. Examples of k-space trajectories for designs with $r = 0.1$, $r = 0.56$, and the sinusoidal design are given in (c), (d), and (e) respectively. Note the similarities in trajectories between the trapezoidal design with $r = 0.56$ (d) and the sinusoidal design (e). The corresponding k-space sampling densities for these designs ($r = 0.1$, $r = 0.56$, and sinusoidal) are given in (f), (g), and (h) respectively. An example of a 2-interleave trajectory ($r = 0.50$) is shown in (i).

h

i

k_y

k_x

k_y

k_x

k_x
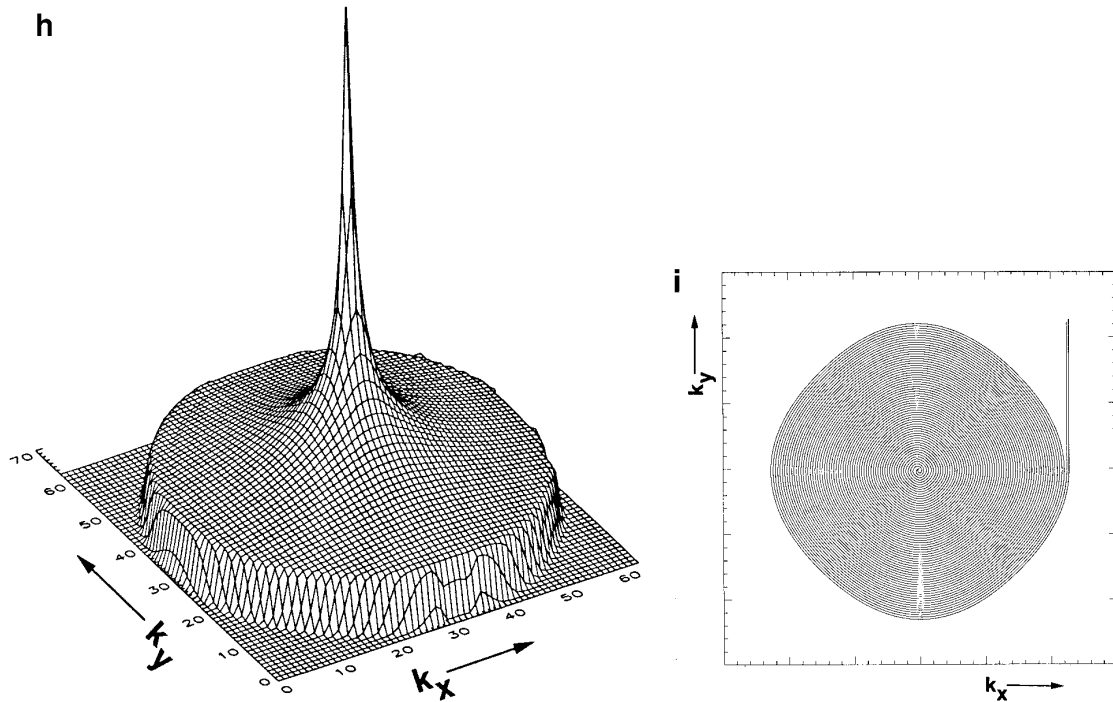
FIG. 1—*Continued*

RESULTS AND DISCUSSION

Figures 2a and 2b show a comparison of the image quality for the standard sinusoidal waveform design and the trapezoidal design with $r = 0.56$. The minimal visible difference between Figs. 2a and 2b suggests that image quality was preserved with the trapezoidal design, despite the differences in trajectory, and the potentially larger eddy-current effects associated with trapezoidal waveform scanning. The auto-

correlation analysis of the time-series data confirmed this, showing a virtually identical effective (in-plane) image resolution of 1.377 and 1.376 voxel dimensions for sinusoidal and trapezoidal waveforms, respectively. Also the scan-to-scan stability was similar for both techniques, as indicated by the equivalent distribution of the temporal standard deviation values across the image (Fig. 3).

At the condition $b_1 < a_1$ in Eq. [4], i.e., $r > 1 - \sqrt{1 - 8/\pi^2} = 0.56$, the required SR (at specific T_{acq}) falls below that for sinusoidal waveforms. Alternatively, with r

TABLE 1
Characteristics of Trapezoidal Waveforms as a Function of the Ramp Fraction r, and Compared to a Standard Sinusoidal Waveform

r	Ramp (%)	RMS (%)	Shape (%)	SR_{max} (T/ms)	G_{max} (G/cm)
Sinusoid	100	24	1.5	110	2.00
0.90	90	24	7.6	90	2.27
0.70	70	24	4.9	99	1.95
0.56	56	24	4.5	115	1.80
0.50	50	24	7.8	124	1.76
0.30	30	25	20.0	193	1.63
0.10	10	27	31.5	554	1.57

Note. All waveforms were designed to have $T_{acq} = 22$ ms. Ramp and RMS refer to gradient duty cycles, whereas SR_{max} and G_{max} relate to maximum required slew rate and gradient amplitude respectively. Shape indicates the maximum deviation from circular k-space coverage (see text).

sinusoid **trapezoid**
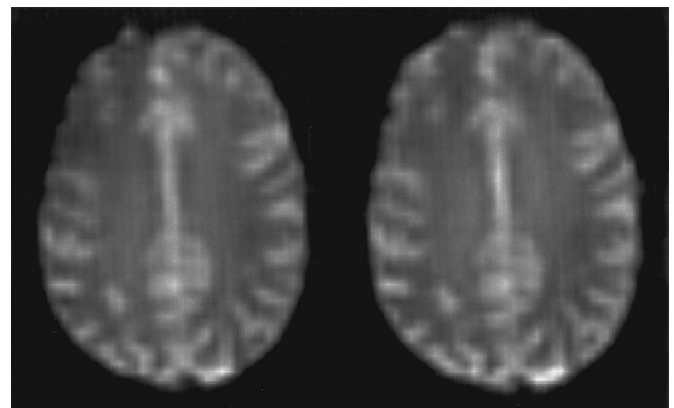
FIG. 2. Comparison of image quality for sinusoidal and trapezoidal spiral scan. For the trapezoidal scan, a ramp fraction $r = 0.56$ was used.
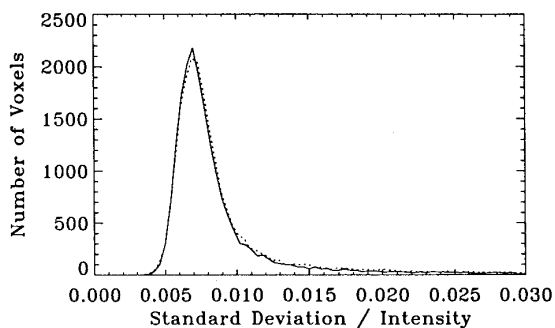
FIG. 3. Histograms of standard deviation of the image intensity time course for sinusoidal (solid line) and trapezoidal (dotted line) spiral waveforms. Note the minimal differences between the two techniques.

< 0.56, one could use the extra available SR to increase the waveform amplitude and reduce T_{acq} (Eq. [2]). The disadvantage is the increased ramping duty cycle, and the increased deviation from circular k-space coverage (Table 1). At $r = 0.5$ one could synchronize the ramps of G_x with the flat tops of G_y (Fig. 1b) and rotate the waveforms $45°$ in the $x–y$ plane, thus gaining a factor of $\sqrt{2}$ in available SR (equivalent to the situation $r = 1.0$). This allows a factor of $2^{0.25} = 1.19$ reduction in T_{acq}, however, with the penalty of a 100% ramping duty cycle. The effects of trapezoidal scanning on gradient coil heating (expressed by RMS in Table 1) are similar to conventional sinusoidal trajectories.

Finally, another potential advantage of trapezoidal gradients is their ease of implementation. Trapezoidal waveforms allow implementation on a wider variety of scanners as compared to sinusoidal waveforms (8), which require tabular representation.

CONCLUSION

Trapezoidal single-shot spiral scanning allows for reduction of either the ramping duty cycle or the duration data acquisition window. This can overcome limitations of the gradient hardware and lead to increased scan speed in, e.g., f MRI experiments.

ACKNOWLEDGMENTS

REFERENCES

1. C. H. Meyer, B. S. Hu, D. G. Nishimura, and A. Macovski, A., Fast spiral coronary artery imaging, *Magn. Reson. Med.* **28,** 202–213 (1992).

2. D. G. Nishimura, P. Irrarrazabal, and C. H. Meyer, A velocity k-space analysis of flow effects in in echo-plannar and spiral imaging, *Magn. Reson. Med.* **33,** 549–556 (1995).

3. G. H. Glover and A. T. Lee, Motion artifacts in f MRI: Comparison of 2DFT with PR and spiral scan methods, *Magn. Reson. Med.* **33,** 624–635 (1995).

4. D. C. Noll, J. D. Cohen, C. H. Meyer, and W. Schneider, Spiral k-space MR imaging of cortical activation, *J. Magn. Reson. Imaging* **5,** 49–56 (1995).

5. Y. Yang, G. H. Glover, P. van Gelderen, V. S. Mattay, A. K. S. Santha, C. T. W. Moonen, D. R. Weinberger, J. A. Frank, and J. H. Duyn, Fast 3D functional magnetic resonance imaging at 1.5 T with spiral acquisition, *Magn. Reson. Med.* **36,** 620–626 (1996).

6. J.-R. Liao, J. M. Pauly, and N. Pelc, MRI using piecewise-linear spiral trajectory, *Magn. Reson. Med.* **38,** 246–252 (1997).

7. A. Macovski and C. Meyer, A novel fast scanning system, *in* ''Proc. Society of Magnetic Resonance in Medicine, Fifth Annual Meeting, 1986 (Works in Progress),'' p. 156–157.

8. J. G. Pipe and A. Haj-Ali, An approximation to spiral imaging using trapezoidal waveforms and collapsing spirals, *in* ''Proc. International Society of Magnetic Resonance in Medicine, Fourth Scientific Meeting, 1996,'' p. 391.

9. C. Salustri, Y. Yang, J. H. Duyn, and G. H. Glover, Comparison between analytical and numerical solutions for spiral trajectory in 2D k-space, *in* ''Proc. International Society of Magnetic Resonance in Medicine, Fifth Scientific Meeting, 1997.''

10. R. S. Likes, Moving gradient Zeugmatography. U.S. Patent 4307343 (1981).

11. Y. Yang, J. A. Frank, G. H. Glover, P. van Gelderen, A. C. Patel, V. S. Mattay, and J. H. Duyn, A comparison of fast MR scan techniques for cerebral activation studies at 1.5 tesla, *Magn. Reson. Med.,* in press.

12. J. I. Jackson, C. H. Meyer, D. G. Nishimura, and A. Macovski, Selection of a convolution function for Fourier inversion using gridding, *IEEE Trans. Med. Imaging* **10,** 473–478 (1991).

13. M. Unser and A. Aldroubi, A multiresolution image registration procedure using spline pyramids, *in* ''Proc. SPIE, San Diego, California, USA, 1993,'' Vol. 2034, pp. 160–170.

14. P. Thevenaz, U. E. Ruttimann, and M. Unser, Iterative multi-scale registration without landmarks, *in* ''Proc. International Conference on Image Processing, Washington, DC, USA, 1995,'' Vol. 3, pp. 228–231.

15. J. Xiong, J. H. Gao, J. L. Lancaster, and P. Fox, Clustered pixel analysis for functional MRI activation studies of the human brain, *Human Brain Mapping* **3,** 287–301 (1995).

16. K. Worsley and K. Friston, Analysis of f MRI time-series revisited—again, *Neuroimaging* **2,** 173–181 (1995).